Published in final edited form as:
Toxicol Appl Pharmacol. 2010 December 1; 249(2): 178–187. doi:10.1016/j.taap.2010.09.005.

Expression of proliferative and inflammatory markers in a full-thickness human skin equivalent following exposure to the model sulfur mustard vesicant, 2-chloroethyl ethyl sulfide

Adrienne T. Black[1], **Patrick J. Hayden**[2], **Robert P. Casillas**[3], **Diane E. Heck**[4], **Donald R. Gerecke**[1], **Patrick J. Sinko**[5], **Debra L. Laskin**[1], and **Jeffrey D. Laskin**[6,*]

[1]Pharmacology and Toxicology, Rutgers University, Piscataway, NJ

[2]MatTek Corporation, Ashland, MA

[3]Battelle Memorial Institute, Columbus, OH

[4]Environmental Health Sciences, New York Medical College, Valhalla, NY

[5]Pharmaceutics, Rutgers University, Piscataway, NJ

[6]Environmental and Occupational Medicine, UMDNJ-Robert Wood Johnson Medical School, Piscataway, NJ, USA

Abstract

Sulfur mustard is a potent vesicant that induces inflammation, edema and blistering following dermal exposure. To assess molecular mechanisms mediating these responses, we analyzed the effects of the model sulfur mustard vesicant, 2-chloroethyl ethyl sulfide, on EpiDerm-FT™, a commercially available full-thickness human skin equivalent. CEES (100–1000 μM) caused a concentration-dependent increase in pyknotic nuclei and vacuolization in basal keratinocytes; at high concentrations (300–1000 μM), CEES also disrupted keratin filament architecture in the stratum corneum. This was associated with time-dependent increases in expression of proliferating cell nuclear antigen, a marker of cell proliferation, and poly(ADP-ribose) polymerase (PARP) and phosphorylated histone H2AX, markers of DNA damage. Concentration- and time-dependent increases in mRNA and protein expression of eicosanoid biosynthetic enzymes including COX-2, 5-lipoxygenase, microsomal PGE_2 synthases, leukotriene (LT) A_4 hydrolase and LTC_4 synthase were observed in CEES-treated skin equivalents, as well as in antioxidant enzymes, glutathione *S*-transferases A1–2 (GSTA1–2), GSTA3 and GSTA4. These data demonstrate that CEES induces rapid cellular damage, cytotoxicity and inflammation in full-thickness skin equivalents. These effects are similar to human responses to vesicants *in vivo* and suggest that the full thickness skin equivalent is a useful *in vitro* model to characterize the biological effects of mustards and to develop potential therapeutics.

*To whom correspondence should be addressed, Jeffrey D. Laskin, Ph.D., Department of Environmental and Occupational Medicine, UMDNJ-Robert Wood Johnson Medical School, 170 Frelinghuysen Road Piscataway, NJ, 08854 jlaskin@eohsi.rutgers.edu.

Conflict of Interest statement: One of the authors (P.J. Hayden) is employed by MatTek Corporation, manufacturer of the EpiDerm-FT™ full-thickness skin equivalent used in the experiments. The other authors have no conflicts of interest to declare.

Keywords

vesicant; sulfur mustard; eicosanoids; apoptosis; skin

Introduction

Sulfur mustard is a potent skin vesicant known to cause oxidative stress, inflammation, blistering and persistent tissue damage (Papirmeister *et al.*, 1991; Shakarjian *et al.*, 2009). As a bifunctional alkylating agent, sulfur mustard modifies many tissue components including lipids, proteins and nucleic acids, forming monofunctional adducts and intermolecular cross-links (Debouzy *et al.*, 2002; van der Schans *et al.*, 2002; Mol *et al.*, 2008). Basal keratinocytes appear to be particularly sensitive to sulfur mustard and the blistering process involves apoptosis and necrosis, and detachment from the basement membrane (Papirmeister *et al.*, 1991). This is followed by wound healing, a process by which surviving keratinocytes in adjacent areas migrate into sites of tissue damage and regenerate the epidermal layers of the skin. A variety of factors regulate the response of the skin to sulfur mustard including dose and duration of exposure, persistence in the tissue, the generation of reactive metabolites, and the activity of antioxidant defense and detoxification pathways. Turnover of damaged cells in the epidermis following sulfur mustard exposure can also contribute to the wound healing response.

Most studies on the mechanism of action of sulfur mustard have used animal models including mice, guinea pigs, pigs and rabbits (Dannenberg *et al.*, 1985; Harada *et al.*, 1987; Monteiro-Riviere and Inman, 1997; Monteiro-Riviere *et al.*, 1999; Babin *et al.*, 2000; Reid *et al.*, 2000; Dachir *et al.*, 2002; Dachir *et al.*, 2004; Wormser *et al.*, 2004a; Pal *et al.*, 2009; Tewari-Singh *et al.*, 2009; Dachir *et al.*, 2010). While these models recapitulate many of the actions of sulfur mustard in human skin including inflammation, necrosis and wound repair, gross blistering, a major response following human exposure is not observed (Smith *et al.*, 1997a). This has limited the utility of animal models for the development of dermal pharmaco-therapeutics.

In vitro models have also been used to investigate the cytotoxic actions of sulfur mustard including human skin explants, isolated human and mouse epidermal keratinocytes, and keratinocyte cell lines (Smith *et al.*, 1990; Cowan *et al.*, 2002; Lefkowitz and Smith, 2002; Dillman *et al.*, 2003; Dillman *et al.*, 2004; Gross *et al.*, 2006; Shakarjian *et al.*, 2006; Simbulan-Rosenthal *et al.*, 2006; Rebholz *et al.*, 2008; Black *et al.*, 2010; Tewari-Singh *et al.*, 2010). Using these models, sulfur mustard-induced cell signaling pathways have been identified, and DNA and antioxidant modifications characterized (Dillman *et al.*, 2004; Rebholz *et al.*, 2008; Black *et al.*, 2010). However, these systems are also limited in their utility since they do not resemble differentiated keratinocytes in the skin.

Of recent interest is the development of *in vitro* human skin equivalents that more closely resemble human skin (Ponec *et al.*, 2002; Hayden *et al.*, 2003). These models, referred to as full-thickness skin equivalents, consist of primary human epidermal keratinocytes grown on membrane supports in the absence and presence of a dermal substratum such as primary human fibroblasts embedded in an artificial extracellular matrix. Keratinocytes within these skin equivalents differentiate, forming distinct basal, spinous and granular layers, as well as a stratum corneum, when placed at an air-liquid interface. In addition to expressing a number of differentiation markers including involucrin, K1/K10 cytokeratins, and type I epidermal transglutaminase, full-thickness skin equivalents also form a well defined basement membrane overlaying the dermal component (Boelsma *et al.*, 2000; Ponec *et al.*, 2002). These models have also been reported to express many of the genes encoding

xenobiotic metabolizing enzymes found in human skin, including phase I and phase II enzymes (Luu-The *et al.*, 2009; Hu *et al.*, 2010).

Full-thickness skin equivalents have been shown to be highly sensitive to exposure to sulfur mustard and the related vesicant, 2-chloroethyl ethyl sulfide (CEES), which readily induce microblister formation and associated structural damage to basal keratinocytes (Blaha *et al.*, 2000b; Blaha *et al.*, 2001; Hayden *et al.*, 2009). CEES treatment also results in the release of inflammatory proteins including interleukin-1 (IL-1) α, prostaglandin E_2 and IL-1 receptor antagonist (Blaha *et al.*, 2000b). In the present studies, we used a full-thickness skin equivalent to further characterize the effects of CEES on keratinocyte DNA damage and expression of antioxidants and enzymes that generate inflammatory mediators. Our data provide support for the use of this human skin equivalent model for investigating mechanisms of sulfur mustard-induced toxicity and developing effective countermeasures.

Materials and Methods

Reagents

Rabbit polyclonal anti- poly(ADP-ribose) polymerase (PARP) antibody was purchased from Cell Signaling Technology (Beverly, MA), anti-proliferating cell nuclear antigen (PCNA) and anti-cyclooxygenase-2 (COX-2) antibodies from Abcam (Cambridge, MA), anti-5-lipooxygenase (5-LOX) antibody from Cayman Chemical (Ann Arbor, MI), and anti-phospho-histone H2AX antibodies from R&D systems (Minneapolis, MN) or Cell Signaling Technology (Beverly, MA). Rabbit polyclonal antibodies to leukotriene A_4 hydrolase (LTA_4 hydrolase), goat polyclonal antibodies to β-actin, and horseradish peroxidase-labeled donkey anti-goat secondary antibodies were from Santa Cruz Biotechnology (Santa Cruz, CA). Horseradish peroxidase-labeled goat anti-rabbit secondary antibodies and detergent-compatible protein assay reagents were from Bio-Rad Laboratories (Hercules, CA). Rabbit IgG was from ProSci (Poway, CA) and the Vectastain Rabbit Kit and the Peroxidase Substrate Kit DAB from Vector Labs (Burlingame, CA). Multiscribe Reverse Transcriptase was from Promega Corporation (Madison, WI), the RNeasy purification kit from Qiagen (Minneapolis, MN), precast gradient polyacrylamide gels from Pierce Biotechnology, Inc. (Rockford, IL), and the Western Lightning Enhanced Chemiluminescence (ECL) kit from Perkin Elmer Life Sciences, Inc. (Boston, MA). SYBR Green Master Mix and other PCR reagents were purchased from Applied Biosystems (Foster City, CA). CEES, protease inhibitor cocktail, and all other chemicals were from Sigma-Aldrich (St. Louis, MO).

Treatment of skin equivalents

EpiDerm-FT™ full-thickness human skin equivalents (EFT-400) and EFT-400-MM (medium supplemented with growth factors, hormones and lipid precursors) were kindly provided by MatTek Corporation (Ashland, MA). The skin equivalents were placed in 6-well plates in 2 ml of EFT-400-MM. After overnight incubation at 37° C in a humidified incubator, 1 ml of PBS containing vehicle control or CEES was added to the apical surface of the tissues. The cultures were then incubated at 37°C. A stock CEES solution (100 mM) was prepared fresh in absolute ethanol immediately before use and diluted to the appropriate concentrations in PBS. After 2 hr, the skin equivalents were removed from the plates, washed in PBS, immediately placed in the same 6-well culture dishes and incubated for the indicated times. Analysis of the effects of CEES on Epiderm-FT™ was performed in four independent experiments

Tissues were then harvested and stored at 4°C in 3% paraformaldehyde in PBS supplemented with 2% sucrose. For histological and immunohistochemical analysis, tissues were removed from the supports and transferred to 50% ethanol and then paraffin

embedded. Tissue sections (5 μm) were stained with hematoxylin and eosin (H&E) or Gomori One-Step Trichrome stain, followed by counterstaining with aniline blue (Goode Histolabs, New Brunswick, NJ). Specimens were analyzed by light microscopy using ProgRes Capture v2.5 software. For immunohistochemistry, tissue sections were deparaffinized, blocked in 5% or 100% serum at room temperature for 2 hr, and then incubated for 30 min at room temperature or overnight at 4°C with rabbit IgG control, a 1:250 dilution of PCNA or PARP antibodies, 1:100 dilution of phospho-H2AX antibodies or a 1:400 dilution of COX-2 antibodies. The sections were then incubated for 30 min at room temperature. Binding was visualized using a Peroxidase Substrate Kit. In some experiments, the epidermis was removed from unfixed skin equivalents by gentle peeling and immediately used for either mRNA or protein analysis.

Western blotting

Epidermal sheets were lysed in buffer containing 50 mM Tris-HCl pH 8.0, 150 mM NaCl and 1% Triton X-100 supplemented with 5 μl protease inhibitor cocktail which consisted of 4-(2-aminoethyl)benzenesulfonyl fluoride, aprotinin, bestatin hydrochloride, N-(trans-epoxysuccinyl)-L-leucine 4-guanidinobutylamide, EDTA and leupeptin. Proteins (20 μg) from lysates were separated on 10% or precast 4–20% gradient SDS-polyacrylamide gels and then transferred to nitrocellulose membranes. After incubation in blocking buffer (5% dry milk Tris-buffered saline containing 0.1% Tween 20) for 1 hr at room temperature, the membranes were incubated overnight at 4°C with primary antibodies (PCNA, 1:200 dilution; PARP, phospho-H2AX and COX-2, 1:1000 dilutions; 5-LOX, 1:7500 dilution; or LTA_4 hydrolase, 1;1500 dilution) followed by horseradish peroxidase-conjugated secondary antibodies for 1 hr at room temperature. Protein expression was visualized using ECL reagents. Densitometric analysis of western blots was performed using Adobe Photoshop CS2 (Adobe Systems Inc., San Jose, CA) and results are reported in arbitrary units.

Real-time polymerase chain reaction (PCR)

For analysis of mRNA by RT-PCR, each point was analyzed in triplicate. RNA was isolated from the epidermis using an RNeasy purification kit following the manufacturer's protocol. RNA was converted to cDNA using a Multiscribe reverse transcriptase and diluted 1:10 in RNase-DNase-free water for PCR analysis. For each gene to be tested, a standard curve composed of a serial dilution of pooled cDNA from the samples was used as a reference. All values were normalized to GAPDH (n = 3). The control was assigned a value of one and treated samples calculated relative to control. Real-time PCR was performed on an ABI Prism 7300 Sequence Detection System using 96-well optical reaction plates. SYBR-Green was used for detection of fluorescent signal and the standard curve method was used for relative quantification analysis. The primer sequences for the genes were generated using Primer Express software (Applied Biosystems) and the oligonucleotides synthesized by Integrated DNA Technologies, Inc. (Coralville, IA). The forward and reverse sequences (5' → 3') were: COX-2, GCCTGATGATTGCCCGACT and GCTGGCCCTCGCTTATGATCT; FLAP, AAGTGGAGCACGAAAGCAGG and CGGTCCTCTGGAAGCTCCTC; GAPDH, TGGGCTACACTGAGCACCAG and GGGTGTCGCTGTTGAAGTCA; GSTA1–2, TTGATGTTCCAGCAAGTGCC and CACCAGCTTCATCCCATCAAT; GSTA3, TTCTGCCCTTATGTCGACCTG and TGATCAAGGCAATCTTGGCAT; GSTA4, GCTCCACTATCCCAACGGAA and AAAACCCATCTCACGGACTCC; 5-LOX, TCGAGTTCCCCTGCTACCG and TCAGGACAACCTCGACATCG; LTA_4 hydrolase, TGAAGTTTACCCGGCCCTTA and GGATTTGTCAAAGGCAGCA; LTC_4synthase, AGTACTTCCCGCTGTTCCTCG and GAAAGAAGATGCCGGCGAC; mPGES-1, CACCGGAACGACATGGAGAC and GACGAAGCCCAGGAAAAGG; mPGES-2, GATGTACGTGGTGGCCATCA and CTCTTCTTCCGCAGCCTCAC; Cu,Zn-SOD, GTCGTAGTCTCCTGCAGCGTC and

CTGGTTCCGAGGACTGCAA; and Mn-SOD, TCTGGACAAACCTCAGCCCT and GCAACTCCCCTTTGGGTTCT.

Statistical analysis

Data are expressed as mean ± SEM. Statistical differences between the means were determined using two-way ANOVA and were considered significant at $p < 0.05$.

Results

Effects of CEES on skin structure

In initial studies, we assessed structural alterations in full-thickness human skin equivalents following CEES administration. H&E staining of control tissue showed a stratified epidermal layer containing both basal keratinocytes and differentiated suprabasal cells including prominent granular cells and a thick stratum corneum (Fig. 1A). Following exposure to CEES (100 – 1000 μM), an increase in the number of pyknotic nuclei and cytoplasmic vacuolization was evident in basal keratinocytes (Figs. 1A and 2). In the stratum corneum from both control and CEES (100 μM)-treated skin equivalents, prominent trichrome staining was detected (Fig. 1B). However, a marked decrease in staining was noted with 300 μM and 1000 μM CEES (Fig. 1B). These data indicate that CEES causes a dose-related disruption of the keratin filament structure in the stratum corneum.

Effects of CEES on markers of cell proliferation and DNA damage

PCNA is a DNA polymerase cofactor important in both DNA synthesis and repair (Moldovan *et al.*, 2007). Immunohistochemistry revealed that PCNA was constitutively expressed in basal keratinocytes in the skin equivalent. CEES treatment resulted in a time-dependent increase in expression of PCNA which reached a maximum after 6–24 hr with 1000 μM CEES; subsequently, levels decreased, and by 72 hr were at control levels (Fig. 3). PCNA was detected largely in basal keratinocytes and in fibroblasts. Western blot analysis of lysates from epidermal sheets isolated from the skin equivalents indicated that PCNA was constitutively expressed in keratinocytes. Expression of the protein was upregulated as early as 15 min post-exposure, persisting for at least 24 hr (Fig. 4). Maximal protein expression was evident with 300–1000 μM CEES (Fig. 4).

The DNA repair enzyme, PARP, was also constitutively expressed in skin equivalents (Debiak *et al.*, 2009). Treatment with CEES (1000 μM) increased PARP expression within 2–6 hr, mainly in basal keratinocytes (Fig. 5). These effects were transient, with little to no staining detectable at 72 hr post-CEES treatment. PARP protein was also upregulated 15 min, 6 hr and 24 hr following CEES treatment with maximum expression at 1000 μM CEES (Fig. 4).

Phosphorylated histone H2AX (phospho-H2AX) is key for the repair of double-strand DNA breaks (Mah *et al.*, 2010). Low constitutive expression of phospho-H2AX was evident in the granular keratinocyte layer of the epidermis in the skin equivalents (Fig. 6). Treatment with 1000 μM CEES resulted in a rapid increase in expression of phospho-H2AX in basal keratinocytes with a maximum at 2–6 hr. In the granular layer, phospho-H2AX protein continued to increase up to 72 hr. Western blot analysis of the tissue confirmed that phospho-H2AX protein expression increased 24 hr following CEES treatment. Maximum levels were evident with 100–1000 μM CEES (Fig. 4).

Effects of CEES on expression of enzymes that mediate eicosanoid production

A characteristic response of the skin to irritants is upregulation of COX-2, the rate-limiting enzyme in the production of prostaglandins (Fitzpatrick, 2004). Treatment of skin

equivalents with CEES caused a time and dose-dependent increase in COX-2 expression; maximal increases were observed 6 hr post-treatment with 1000 μM of the vesicant (Fig. 7). At early time points (2 hr), COX-2 expression was detected largely in fibroblasts, while subsequently (6 hr), the protein was also evident in keratinocytes (Fig. 7). CEES (100–1000 μM) also upregulated expression of COX-2 mRNA and protein at 6 hr and 24 hr post-treatment as determined by real-time PCR and Western blot analysis of lysates from epidermal sheets isolated from the skin equivalents (Figs. 4 and 8).

Oxidation of arachidonic acid by COX-2 generates prostaglandin PGH_2, which is converted to PGE_2 by at least two microsomal PGE_2 synthases, mPGES-1 and mPGES-2 (Murakami *et al.*, 2002). CEES (100–1000 μM) treatment of skin equivalents resulted in a 2-fold increase in mRNA expression of mPGES-1 and mPGES-2, which was observed 24 hr post-exposure. Expression of mPGES-1, but not mPGES-2, was also upregulated 6 hr post-treatment (Fig. 8).

Leukotrienes are generated via the actions of 5-LOX and 5-LOX activating protein (FLAP) (Funk, 2001). Products include leukotriene A_4 (LTA_4) which is converted to leukotriene B_4 (LTB_4) and leukotriene C_4 (LTC_4) by LTA_4 hydrolase and LTC_4 synthase, respectively (Funk, 2001). Increased mRNA expression of 5-LOX (3–4-fold at 6 and 24 hr), but not FLAP, was detected in the skin equivalents following CEES treatment (Fig. 8 and not shown). LTA_4 hydrolase and LTC_4 synthase mRNA were also upregulated 2–3-fold after 6 hr and 24 hr (Fig. 8). This was correlated with increased expression of 5-LOX and LTA_4 hydrolase protein at 6 hr and 24 hr post-CEES treatment (Fig. 4).

Effects of CEES on expression of primary and secondary antioxidant enzymes

In further studies, we determined if CEES exposure altered antioxidant enzyme expression in the full-thickness skin equivalents. CEES (100–1000 μM) treatment resulted in a 2-fold increase in mRNA expression of Cu,Zn-SOD after 24 hr (Fig. 9). In contrast, Mn-SOD mRNA expression decreased rapidly (6 hr) after CEES (Fig. 9). The glutathione *S*-transferase (GST) superfamily of secondary antioxidant enzymes, in particular, members of the GST alpha (GSTA) subfamily, are critical mediators in the detoxification of oxidized macromolecules via glutathione conjugation (Hayes *et al.*, 2004). Figure 9 shows that CEES treatment of human skin equivalents resulted in increased mRNA expression of GSTA1–2 (4-fold at 6 and 24 hr), GSTA3 (3–6-fold at 6 hr and 24 hr) and GSTA4 (4-fold at 6 and 24 hr).

Discussion

Sulfur mustard has been shown to injure basal keratinocytes in humans and in animal models, inducing chromatin condensation and cytoplasmic vacuolization followed by cellular swelling and loss of cell membrane integrity (Papirmeister *et al.*, 1991; Smith *et al.*, 1995; Smith *et al.*, 1998; Rice, 2003; Shakarjian *et al.*, 2009). This results in microblister formation at the dermal-epidermal junction and, in some cases, separation of the epidermis from the dermis (Smith *et al.*, 1997a). Consistent with these studies, we found that CEES treatment of the full-thickness human skin equivalent results in the formation of pyknotic nuclei and vacuolization in basal keratinocytes. These morphologic changes are directly linked to blister formation in human skin (Proskuryakov *et al.*, 2003), suggesting that the full-thickness human skin equivalent model is useful in recapitulating the *in vivo* dermal responses of humans to vesicants. Trichrome staining of CEES-treated full-thickness skin equivalents also revealed alterations in keratin organization in the stratum corneum. These results are in agreement with earlier studies demonstrating that vesicants induce keratin aggregation and abnormal filament assembly and can directly modify cytoskeletal proteins including cytokeratins 5, 6, 9, 14 and 16, actin and annexin A2 (Dillman *et al.*, 2003; Hess

and FitzGerald, 2007; Mol *et al.*, 2008; Sayer *et al.*, 2009). Single amino acid mutations in keratin 5 and keratin 14 can perturb filament assembly, resulting in skin blistering diseases (Uitto *et al.*, 2007). Sulfur mustard-induced modifications in keratins 5 and 14 are thought to lead to alterations in hemidesmosomes which attach basal keratinocytes to the basement membrane (Dillman *et al.*, 2003). Further studies are needed to determine if these keratins are similarly modified in skin equivalents and if this can lead to the detachment of keratinocytes from the dermal-epidermal junction. It should be noted that the stratum corneum is also key for maintaining the barrier functions of the skin; disruption of the cytokeratin architecture by vesicants may interfere with this activity, contributing to toxicity. In this regard, sulfur mustard has been reported to increase transepidermal water loss in both animal and *in vitro* models (Graham *et al.*, 2002; Dachir *et al.*, 2010).

DNA is a major target for sulfur mustard and related vesicants and is readily modified by the formation of both monofunctional and bifunctional adducts, generating apurinic sites and strand breaks (Papirmeister *et al.*, 1991). In response to DNA damage, several key biochemical pathways are activated which are important in protecting cells against injury and initiating repair processes. For example, following CEES administration, phosphorylation of the DNA damage sensors, ataxia telangiectasia-mutated (ATM) and ataxia telangiectasia-RAD-3-related (ATR) proteins is observed, as well as check point kinases 1 and 2, and the down-stream cell cycle regulatory proteins, cdc25A, cdc25C and cdk2 (Tewari-Singh *et al.*, 2010). PCNA, a DNA polymerase cofactor that promotes DNA replication, is also increased in mouse and pig skin following sulfur mustard or CEES exposure (Smith *et al.*, 1997b; Tewari-Singh *et al.*, 2009). Similarly, we found that CEES treatment of the full-thickness skin equivalent model results in increased PCNA expression which was evident in histology sections and in western blots of isolated epidermis. Increased PARP expression was also detected. PARP is a NAD+-dependent nuclear enzyme activated in response to single- and double-strand DNA breaks (Debiak *et al.*, 2009). Following activation, PARP binds to DNA and (ADP-ribosyl)ates itself, as well as many other proteins involved in DNA repair and chromatin remodeling. Previous studies have shown that PARP is rapidly activated by sulfur mustard and CEES in guinea pig skin and in cultured keratinocytes (Hinshaw *et al.*, 1999; Bhat *et al.*, 2000; Kan *et al.*, 2003; Bhat *et al.*, 2006; Tewari-Singh *et al.*, 2010). Moreover, inhibition of PARP suppresses DNA repair in sulfur mustard-treated human keratinocytes, demonstrating that activation of this enzyme is involved in this process. It has also been suggested that PARP may indirectly contribute to sulfur mustard toxicity. According to this “PARP hypothesis”, sulfur mustard-induced DNA adducts impair the replication process, resulting in extensive DNA strand breaks and activation of PARP. Subsequent activation of PARP can lead to rapid depletion of intracellular stores of pyridine nucleotides and, consequently, inhibition of ATP production resulting in cell death (Papirmeister *et al.*, 1985; Papirmeister *et al.*, 1991). Whether PARP contributes to toxicity or wound healing may depend on doses and duration of exposure to sulfur mustard.

H2AX is rapidly phosphorylated following double-strand DNA breaks and is key in activating DNA damage response pathways important in repair (Mah *et al.*, 2010). Following CEES treatment, increased phosphorylation of H2AX was detected in the nuclei of basal cells of the full-thickness human skin equivalents, confirming DNA damage. Interestingly, low constitutive expression of phosphorylated H2AX was also evident in granular layers of the skin equivalents, and this increased after CEES administration. In contrast to nuclear localization in basal cells, in granular cells, phosphorylated H2AX was distributed throughout the cytoplasm. Granular keratinocytes are known to undergo terminal differentiation and form the stratum corneum; during this process, the nuclear membrane and the DNA degrade and this may underlie nuclear delocalization of H2AX (Houben *et al.*, 2007). Thus, increased phosphorylated H2AX in the granular layer post-CEES treatment

may result from increases in expression of this protein in individual keratinocytes and in the number of cells undergoing differentiation. Increased levels of phoshorylated-H2AX have also been described in human fibroblasts and Chinese hamster cells following exposure to DNA alkylating agents including cisplatin and nitrogen mustard (Clingen *et al.*, 2008), and human keratinocytes treated with sulfur mustard (Miller *et al.*, 2010).

Accumulating evidence suggests that the toxicity of vesicants involves the generation of reactive oxygen species (ROS) and induction of oxidative stress (Laskin *et al.*, 2010). This is associated with increased expression of antioxidant enzymes, which function to limit cytotoxicity (Droge, 2002). We have recently reported that CEES stimulates ROS generation by mouse keratinocytes and induces protein oxidation (Black *et al.*, 2010). This was correlated with increased expression of a number of antioxidant enzymes including Cu,Zn-SOD, thioredoxin reductase, catalase, GSTA1–2 and GST-P1. Increased protein and DNA oxidation have also been described in CEES-treated mouse skin (Pal *et al.*, 2009). The present studies demonstrate that CEES similarly alters expression of antioxidants in full-thickness human skin equivalents. Thus, while increases in Cu,Zn-SOD expression were evident 24 hr after CEES treatment, a small decrease in Mn-SOD was noted after 6 hr. GSTA1–2, GSTA3 and GSTA4 mRNA were also upregulated after 6 and 24 hr. Cu,Zn-SOD is a cytosolic enzyme, while Mn-SOD is localized in the mitochondria (Droge, 2002). Sulfur mustard exposure is known to selectively damage mitochondria and this may result in decreased Mn-SOD expression (Shahin *et al.*, 2001; Gould *et al.*, 2009). Antioxidants including SOD are known to play a role in protecting cells from oxidative DNA damage and previous studies have shown that pretreatment of guinea pigs with Mn-SOD or Cu,Zn-SOD reduce sulfur mustard-induced skin damage (Eldad *et al.*, 1998). Our findings of increased expression of Cu,Zn-SOD after CEES treatment are consistent with this protective role in full-thickness human skin equivalents. Earlier work has also shown that sulfur mustard increases total GST activity in human keratinocytes (Gross *et al.*, 2006). GSTs constitute a large superfamily of detoxification enzymes that conjugate glutathione to oxidized cellular macromolecules, a process that increases their elimination from cells (Hayes *et al.*, 2004). The GST alpha (GSTA) family of enzymes is known to remove lipid hydroperoxides, thereby breaking radical-forming chain reactions (Hayes *et al.*, 2004). Increases in expression of GSTA enzymes following CEES exposure may be important in protecting keratinocyte membranes from lipid peroxide-induced damage.

Hallmarks of sulfur mustard-induced skin toxicity include erythema, edema and pruritis (Rice, 2003). This is accompanied by increased production of eicosanoids (Shakarjian *et al.*, 2009). Sulfur mustard and CEES have been reported to upregulate expression of COX-2, the rate-limiting enzyme in prostaglandin biosysnthesis, in mouse skin (Nyska *et al.*, 2001) and in mouse keratinocytes grown at an air-liquid interface (Black *et al.*, 2010). Consistent with these results, we found that COX-2 mRNA and protein expression were increased in the full-thickness skin equivalent following CEES treatment, suggesting that this enzyme plays a key role in mediating dermal inflammation and injury following vesicant exposure. This is supported by findings that sulfur mustard-induced skin injury and inflammation are reduced in COX-2 deficient mice and in mice treated with topical inhibitors of cyclooxygenase activity (Babin *et al.*, 2000; Casillas *et al.*, 2000; Dachir *et al.*, 2002; Dachir *et al.*, 2004; Wormser *et al.*, 2004b). In full-thickness skin equivalents, CEES was also found to upregulate mPGES-1 and mPGES-2 mRNA expression, two prostanoid synthases downstream of COX-2 that generate PGE_2, a key mediator in the development of dermal inflammatory responses (Murakami *et al.*, 2002). Increased PGE_2 production has been reported in sulfur mustard-treated human skin explants and mouse skin (Rikimaru *et al.*, 1991; Dachir *et al.*, 2004), as well as in CEES-treated full-thickness human skin equivalents (Blaha *et al.*, 2000a; Blaha *et al.*, 2000b). Our findings that COX-2, mPGES-1 and mPGES-2 are coordinately upregulated in the human full thickness skin equivalent

following CEES treatment suggest a potentially important mechanism for the generation of PGE_2 in the skin following vesicant exposure. 5-LOX, LTA_4 hydrolase and LTC_4 synthase, enzymes responsible for the synthesis of LTB_4 and LTC_4, were also upregulated in the skin equivalents after CEES exposure. These results are in agreement with previous findings on the effects of CEES in mouse keratinocytes grown at an air-liquid interface (Black *et al.*, 2010), and that sulfur mustard increases LTB_4 levels in inflammatory lesions in rabbit skin (Tanaka *et al.*, 1997). Additional studies correlating eicosanoid biosynthetic enzyme gene and protein expression with enzymatic activity and production of prostaglandins and leukotrienes in the full-thickness human skin equivalent will be important in assessing the role of these mediators in vesicant-induced inflammation and injury.

In summary, the present studies demonstrate the utility of the full-thickness human skin equivalent model to investigate mechanisms of vesicant-induced skin toxicity and for the development of countermeasures. Vesicants can be applied directly to the stratum corneum on the air surface, which more accurately reflects human exposure. Moreover, vesicants generate basal cell damage generally similar to that observed in human skin. Markers for DNA damage in both basal and granular layers of the full thickness skin equivalents were evident, as well as increased expression of mediators that regulate inflammation and wound repair including enzymes that generate arachidonic acid-derived lipid mediators. We also observed changes in expression of antioxidants that may be important in protecting keratinocytes from oxidative stress. At the present time, there are few effective countermeasures against vesicant-induced dermal toxicity. Vesicant-induced changes in the full thickness human skin equivalent model may provide important leads in identifying effective therapeutic strategies. The fact that the skin equivalents are an *in vitro* model will also allow a better understanding of the mechanisms of vesicant toxicity as well as early development of drugs to counter toxicity without the use of animal models.

Acknowledgments

This research was supported by the CounterACT Program, National Institutes of Health Office of the Director, and the National Institute of Arthritis and Musculoskeletal and Skin Diseases, Grant number U54AR055073. Its contents are solely the responsibility of the authors and do not necessarily represent the official views of the federal government. This work was also supported in part by National Institutes of Health grants CA100994, CA093798, CA132624, AR055073, ES004738, ES005022, GM034310, AI084138 and AI51214.

List of Abbreviations

(CEES)	2-chloroethyl ethyl sulfide
(COX-2)	cyclooxygenase-2
(GST)	glutathione *S*-transferase
(LTA_4)	leukotriene A_4
(LTC_4)	leukotriene C_4
(5-LOX)	5-lipoxygenase
(FLAP)	5-LOX activating protein
(phospho-H2AX)	phosphorylated histone H2AX
(PARP)	poly(ADP-ribose) polymerase
(PCNA)	proliferating cell nuclear antigen
(PGE_2)	prostaglandin E_2

(mPGES-1)	microsomal PGE_2 synthase-1
(mPGES-2)	microsomal PGE_2 synthase-2
(SOD)	superoxide dismutase

References

Babin MC, Ricketts K, Skvorak JP, Gazaway M, Mitcheltree LW, Casillas RP. Systemic administration of candidate antivesicants to protect against topically applied sulfur mustard in the mouse ear vesicant model (MEVM). J Appl Toxicol 2000;20(Suppl 1):S141–144. [PubMed: 11428627]

Bhat KR, Benton BJ, Ray R. Poly (ADP-ribose) polymerase (PARP) is essential for sulfur mustard-induced DNA damage repair, but has no role in DNA ligase activation. J Appl Toxicol 2006;26:452–457. [PubMed: 16906506]

Bhat KR, Benton BJ, Rosenthal DS, Smulson ME, Ray R. Role of poly(ADP-ribose) polymerase (PARP) in DNA repair in sulfur mustard-exposed normal human epidermal keratinocytes (NHEK). J Appl Toxicol 2000;20(Suppl 1):S13–17. [PubMed: 11428624]

Black AT, Joseph LB, Casillas RP, Heck DE, Gerecke DR, Sinko PJ, Laskin DL, Laskin JD. Role of MAP kinases in regulating expression of antioxidants and inflammatory mediators in mouse keratinocytes following exposure to the half mustard, 2-chloroethyl ethyl sulfide. Toxicol Appl Pharmacol 2010;245:352–360. [PubMed: 20382172]

Blaha M, Bowers W Jr. Kohl J, DuBose D, Walker J. IL-1-related cytokine responses of nonimmune skin cells subjected to CEES exposure with and without potential vesicant antagonists. In Vitr Mol Toxicol 2000a;13:99–111. [PubMed: 11031321]

Blaha M, Bowers W Jr. Kohl J, DuBose D, Walker J, Alkhyyat A, Wong G. Effects of CEES on inflammatory mediators, heat shock protein 70A, histology and ultrastructure in two skin models. J Appl Toxicol 2000b;20(Suppl 1):S101–108. [PubMed: 11428619]

Blaha M, Kohl J, DuBose D, Bowers W Jr. Walker J. Ultrastructural and histological effects of exposure to CEES or heat in a human epidermal model. In Vitr Mol Toxicol 2001;14:15–23. [PubMed: 11689153]

Boelsma E, Gibbs S, Faller C, Ponec M. Characterization and comparison of reconstructed skin models: morphological and immunohistochemical evaluation. Acta Derm Venereol 2000;80:82–88. [PubMed: 10877124]

Casillas RP, Kiser RC, Truxall JA, Singer AW, Shumaker SM, Niemuth NA, Ricketts KM, Mitcheltree LW, Castrejon LR, Blank JA. Therapeutic approaches to dermatotoxicity by sulfur mustard. I. Modulaton of sulfur mustard-induced cutaneous injury in the mouse ear vesicant model. J Appl Toxicol 2000;20(Suppl 1):S145–151. [PubMed: 11428628]

Clingen PH, Wu JY, Miller J, Mistry N, Chin F, Wynne P, Prise KM, Hartley JA. Histone H2AX phosphorylation as a molecular pharmacological marker for DNA interstrand crosslink cancer chemotherapy. Biochem Pharmacol 2008;76:19–27. [PubMed: 18508035]

Cowan FM, Broomfield CA, Smith WJ. Suppression of sulfur mustard-increased IL-8 in human keratinocyte cell cultures by serine protease inhibitors: implications for toxicity and medical countermeasures. Cell Biol Toxicol 2002;18:175–180. [PubMed: 12083423]

Dachir S, Cohen M, Fishbeine E, Sahar R, Brandies R, Horwitz V, Kadar T. Characterization of acute and long-term sulfur mustard-induced skin injuries in hairless guinea-pigs using non-invasive methods. Skin Res Technol 2010;16:114–124. [PubMed: 20384890]

Dachir S, Fishbeine E, Meshulam Y, Sahar R, Amir A, Kadar T. Potential anti-inflammatory treatments against cutaneous sulfur mustard injury using the mouse ear vesicant model. Hum Exp Toxicol 2002;21:197–203. [PubMed: 12099621]

Dachir S, Fishbeine E, Meshulam Y, Sahar R, Chapman S, Amir A, Kadar T. Amelioration of sulfur mustard skin injury following a topical treatment with a mixture of a steroid and a NSAID. J Appl Toxicol 2004;24:107–113. [PubMed: 15052605]

Dannenberg AM Jr. Pula PJ, Liu LH, Harada S, Tanaka F, Vogt RF Jr. Kajiki A, Higuchi K. Inflammatory mediators and modulators released in organ culture from rabbit skin lesions produced in vivo by sulfur mustard. I. Quantitative histopathology; PMN, basophil, and mononuclear cell survival; and unbound (serum) protein content. Am J Pathol 1985;121:15–27. [PubMed: 4050973]

Debiak M, Kehe K, Burkle A. Role of poly(ADP-ribose) polymerase in sulfur mustard toxicity. Toxicology 2009;263:20–25. [PubMed: 18602966]

Debouzy JC, Aous S, Dabouis V, Neveux Y, Gentilhomme E. Phospholipid matrix as a target for sulfur mustard (HD): NMR study in model membrane systems. Cell Biol Toxicol 2002;18:397–408. [PubMed: 12484550]

Dillman JF 3rd, McGary KL, Schlager JJ. Sulfur mustard induces the formation of keratin aggregates in human epidermal keratinocytes. Toxicol Appl Pharmacol 2003;193:228–236. [PubMed: 14644625]

Dillman JF 3rd, McGary KL, Schlager JJ. An inhibitor of p38 MAP kinase downregulates cytokine release induced by sulfur mustard exposure in human epidermal keratinocytes. Toxicol In Vitro 2004;18:593–599. [PubMed: 15251176]

Droge W. Free radicals in the physiological control of cell function. Physiol Rev 2002;82:47–95. [PubMed: 11773609]

Eldad A, Ben Meir P, Breiterman S, Chaouat M, Shafran A, Ben-Bassat H. Superoxide dismutase (SOD) for mustard gas burns. Burns 1998;24:114–119. [PubMed: 9625234]

Fitzpatrick FA. Cyclooxygenase enzymes: regulation and function. Curr Pharm Des 2004;10:577–588. [PubMed: 14965321]

Funk CD. Prostaglandins and leukotrienes: advances in eicosanoid biology. Science 2001;294:1871–1875. [PubMed: 11729303]

Gould NS, White CW, Day BJ. A role for mitochondrial oxidative stress in sulfur mustard analog 2-chloroethyl ethyl sulfide-induced lung cell injury and antioxidant protection. J Pharmacol Exp Ther 2009;328:732–739. [PubMed: 19064720]

Graham JS, Schomacker KT, Glatter RD, Briscoe CM, Braue EH Jr. Squibb KS. Bioengineering methods employed in the study of wound healing of sulphur mustard burns. Skin Res Technol 2002;8:57–69. [PubMed: 12005121]

Gross CL, Nealley EW, Nipwoda MT, Smith WJ. Pretreatment of human epidermal keratinocytes with D, L-sulforaphane protects against sulfur mustard cytotoxicity. Cutan Ocul Toxicol 2006;25:155–163. [PubMed: 16980241]

Harada S, Dannenberg AM Jr. Vogt RF Jr. Myrick JE, Tanaka F, Redding LC, Merkhofer RM, Pula PJ, Scott AL. Inflammatory mediators and modulators released in organ culture from rabbit skin lesions produced in vivo by sulfur mustard. III. Electrophoretic protein fractions, trypsin-inhibitory capacity, alpha 1-proteinase inhibitor, and alpha 1- and alpha 2-macroglobulin proteinase inhibitors of culture fluids and serum. Am J Pathol 1987;126:148–163. [PubMed: 2433944]

Hayden, PJ.; Ayehunie, S.; Jackson, GR.; Kupfer-Lamore, S.; Last, TJ.; Klausner, M.; Kubilus, J. *In vitro* skin equivalent models for toxicity testing. In: Salem, H.; Katz, SA., editors. Alternative Toxicological Methods. CRC Press; Boca Raton: 2003. p. 229-247.

Hayden PJ, Petrali JP, Stolper G, Hamilton TA, Jackson GR Jr. Wertz PW, Ito S, Smith WJ, Klausner M. Microvesicating effects of sulfur mustard on an in vitro human skin model. Toxicol In Vitro 2009;23:1396–1405. [PubMed: 19619636]

Hayes JD, Flanagan JU, Jowsey IR. Glutathione transferases. Annu Rev Pharmacol Toxicol 2004;45:51–88. [PubMed: 15822171]

Hess JF, FitzGerald PG. Treatment of keratin intermediate filaments with sulfur mustard analogs. Biochem Biophys Res Commun 2007;359:616–621. [PubMed: 17548056]

Hinshaw DB, Lodhi IJ, Hurley LL, Atkins KB, Dabrowska MI. Activation of poly [ADP-Ribose] polymerase in endothelial cells and keratinocytes: role in an in vitro model of sulfur mustard-mediated vesication. Toxicol Appl Pharmacol 1999;156:17–29. [PubMed: 10101095]

Houben E, De Paepe K, Rogiers V. A keratinocyte's course of life. Skin Pharmacol Physiol 2007;20:122–132. [PubMed: 17191035]

Hu T, Khambatta ZS, Hayden PJ, Bolmarcich J, Binder RL, Robinson MK, Carr GJ, Tiesman JP, Jarrold BB, Osborne R, Reichling TD, Nemeth ST, Aardema MJ. Xenobiotic metabolism gene expression in the EpiDerm in vitro 3D human epidermis model compared to human skin. Toxicol In Vitro 2010;24:1450–1463. [PubMed: 20350595]

Kan RK, Pleva CM, Hamilton TA, Anderson DR, Petrali JP. Sulfur mustard-induced apoptosis in hairless guinea pig skin. Toxicol Pathol 2003;31:185–190. [PubMed: 12696578]

Laskin JD, Black AT, Jan YH, Sinko PJ, Heindel ND, Heck DE, Laskin DL. Oxidants and antioxidants in the mechanism of sulfur mustard injury. Ann N Y Acad Sci 2010;1203:92–100. [PubMed: 20716289]

Lefkowitz LJ, Smith WJ. Sulfur mustard-induced arachidonic acid release is mediated by phospholipase D in human keratinocytes. Biochem Biophys Res Commun 2002;295:1062–1067. [PubMed: 12135602]

Luu-The V, Duche D, Ferraris C, Meunier JR, Leclaire J, Labrie F. Expression profiles of phases 1 and 2 metabolizing enzymes in human skin and the reconstructed skin models Episkin and full thickness model from Episkin. J Steroid Biochem Mol Biol 2009;116:178–186. [PubMed: 19482084]

Mah LJ, El-Osta A, Karagiannis TC. gammaH2AX: a sensitive molecular marker of DNA damage and repair. Leukemia 2010;24:679–686. [PubMed: 20130602]

Miller AL, Gross CL, Nealley EW, Clark OE, Waraich NK, Rodgers KL, Smith WJ. Different methods to study the genotoxic marker γ-H2AX following sulfur mustard exposure in cultured human skin cells and a skin tissue construct. Proceedings of the U.S. Army Medical Defense Bioscience Review 2010:103.

Mol MA, van den Berg RM, Benschop HP. Proteomic assessment of sulfur mustard-induced protein adducts and other protein modifications in human epidermal keratinocytes. Toxicol Appl Pharmacol 2008;230:97–108. [PubMed: 18342354]

Moldovan GL, Pfander B, Jentsch S. PCNA, the maestro of the replication fork. Cell 2007;129:665–679. [PubMed: 17512402]

Monteiro-Riviere NA, Inman AO. Ultrastructural characterization of sulfur mustard-induced vesication in isolated perfused porcine skin. Microsc Res Tech 1997;37:229–241. [PubMed: 9144635]

Monteiro-Riviere NA, Inman AO, Babin MC, Casillas RP. Immunohistochemical characterization of the basement membrane epitopes in bis(2-chloroethyl) sulfide-induced toxicity in mouse ear skin. J Appl Toxicol 1999;19:313–328. [PubMed: 10513676]

Murakami M, Nakatani Y, Tanioka T, Kudo I. Prostaglandin E synthase. Prostaglandins Other Lipid Mediat 2002;68–69:383–399.

Nyska A, Lomnitski L, Maronpot R, Moomaw C, Brodsky B, Sintov A, Wormser U. Effects of iodine on inducible nitric oxide synthase and cyclooxygenase-2 expression in sulfur mustard-induced skin. Arch Toxicol 2001;74:768–774. [PubMed: 11305779]

Pal A, Tewari-Singh N, Gu M, Agarwal C, Huang J, Day BJ, White CW, Agarwal R. Sulfur mustard analog induces oxidative stress and activates signaling cascades in the skin of SKH-1 hairless mice. Free Radic Biol Med 2009;47:1640–1651. [PubMed: 19761830]

Papirmeister, B.; Feister, AJ.; Robinson, SI.; Ford, RD. Medical Defense Against Mustard Gas: Toxic Mechanisms and Pharmacological Implications. CRC Press, Inc.; Boca Raton, FL: 1991.

Papirmeister B, Gross CL, Meier HL, Petrali JP, Johnson JB. Molecular basis for mustard-induced vesication. Fundam Appl Toxicol 1985;5:S134–149. [PubMed: 2419197]

Ponec M, Boelsma E, Gibbs S, Mommaas M. Characterization of reconstructed skin models. Skin Pharmacol Appl Skin Physiol 2002;15(Suppl 1):4–17. [PubMed: 12476005]

Proskuryakov SY, Konoplyannikov AG, Gabai VL. Necrosis: a specific form of programmed cell death? Exp Cell Res 2003;283:1–16. [PubMed: 12565815]

Rebholz B, Kehe K, Ruzicka T, Rupec RA. Role of NF-kappaB/RelA and MAPK pathways in keratinocytes in response to sulfur mustard. J Invest Dermatol 2008;128:1626–1632. [PubMed: 18200059]

Reid FM, Graham J, Niemuth NA, Singer AW, Janny SJ, Johnson JB. Sulfur mustard-induced skin burns in weanling swine evaluated clinically and histopathologically. J Appl Toxicol 2000;20(Suppl 1):S153–160. [PubMed: 11428629]

Rice P. Sulphur mustard injuries of the skin. Pathophysiology and management. Toxicol Rev 2003;22:111–118. [PubMed: 15071821]

Rikimaru T, Nakamura M, Yano T, Beck G, Habicht GS, Rennie LL, Widra M, Hirshman CA, Boulay MG, Spannhake EW, et al. Mediators, initiating the inflammatory response, released in organ culture by full-thickness human skin explants exposed to the irritant, sulfur mustard. J Invest Dermatol 1991;96:888–897. [PubMed: 1710639]

Sayer NM, Whiting R, Green AC, Anderson K, Jenner J, Lindsay CD. Direct binding of sulfur mustard and chloroethyl ethyl sulphide to human cell membrane-associated proteins; implications for sulfur mustard pathology. J Chromatogr B Analyt Technol Biomed Life Sci 2009;878:1426–1432.

Shahin S, Cullinane C, Gray PJ. Mitochondrial and nuclear DNA damage induced by sulphur mustard in keratinocytes. Chem Biol Interact 2001;138:231–245. [PubMed: 11714481]

Shakarjian MP, Bhatt P, Gordon MK, Chang YC, Casbohm SL, Rudge TL, Kiser RC, Sabourin CL, Casillas RP, Ohman-Strickland P, Riley DJ, Gerecke DR. Preferential expression of matrix metalloproteinase-9 in mouse skin after sulfur mustard exposure. J Appl Toxicol 2006;26:239–246. [PubMed: 16489579]

Shakarjian MP, Heck DE, Gray JP, Sinko PJ, Gordon MK, Casillas RP, Heindel ND, Gerecke DR, Laskin DL, Laskin JD. Mechanisms mediating the vesicant actions of sulfur mustard after cutaneous exposure. Toxicol Sci 2009;114:5–19. [PubMed: 19833738]

Simbulan-Rosenthal CM, Ray R, Benton B, Soeda E, Daher A, Anderson D, Smith WJ, Rosenthal DS. Calmodulin mediates sulfur mustard toxicity in human keratinocytes. Toxicology 2006;227:21–35. [PubMed: 16935404]

Smith KJ, Casillas R, Graham J, Skelton HG, Stemler F, Hackley BE Jr. Histopathologic features seen with different animal models following cutaneous sulfur mustard exposure. J Dermatol Sci 1997a; 14:126–135. [PubMed: 9039976]

Smith KJ, Graham JS, Hamilton TA, Skelton HG, Petrali JP, Hurst CG. Immunohistochemical studies of basement membrane proteins and proliferation and apoptosis markers in sulfur mustard induced cutaneous lesions in weanling pigs. J Dermatol Sci 1997b;15:173–182. [PubMed: 9302645]

Smith KJ, Hurst CG, Moeller RB, Skelton HG, Sidell FR. Sulfur mustard: its continuing threat as a chemical warfare agent, the cutaneous lesions induced, progress in understanding its mechanism of action, its long-term health effects, and new developments for protection and therapy. J Am Acad Dermatol 1995;32:765–776. [PubMed: 7722023]

Smith KJ, Smith WJ, Hamilton T, Skelton HG, Graham JS, Okerberg C, Moeller R, Hackley BE Jr. Histopathologic and immunohistochemical features in human skin after exposure to nitrogen and sulfur mustard. Am J Dermatopathol 1998;20:22–28. [PubMed: 9504665]

Smith WJ, Gross CL, Chan P, Meier HL. The use of human epidermal keratinocytes in culture as a model for studying the biochemical mechanisms of sulfur mustard toxicity. Cell Biol Toxicol 1990;6:285–291. [PubMed: 2147571]

Tanaka F, Dannenberg AM Jr. Higuchi K, Nakamura M, Pula PJ, Hugli TE, Discipio RG, Kreutzer DL. Chemotactic factors released in culture by intact developing and healing skin lesions produced in rabbits by the irritant sulfur mustard. Inflammation 1997;21:251–267. [PubMed: 9187966]

Tewari-Singh N, Gu M, Agarwal C, White CW, Agarwal R. Biological and molecular mechanisms of sulfur mustard analogue-induced toxicity in JB6 and HaCaT Cells: possible role of ataxia telangiectasia-mutated/ataxia telangiectasia-Rad3-related cell cycle checkpoint pathway. Chem Res Toxicol 2010;23:1034–1044. [PubMed: 20469912]

Tewari-Singh N, Rana S, Gu M, Pal A, Orlicky DJ, White CW, Agarwal R. Inflammatory biomarkers of sulfur mustard analog 2-chloroethyl ethyl sulfide-induced skin injury in SKH-1 hairless mice. Toxicol Sci 2009;108:194–206. [PubMed: 19075041]

Uitto J, Richard G, McGrath JA. Diseases of epidermal keratins and their linker proteins. Exp Cell Res 2007;313:1995–2009. [PubMed: 17531221]

van der Schans GP, Noort D, Mars-Groenendijk RH, Fidder A, Chau LF, de Jong LP, Benschop HP. Immunochemical detection of sulfur mustard adducts with keratins in the stratum corneum of human skin. Chem Res Toxicol 2002;15:21–25. [PubMed: 11800593]

Wormser U, Langenbach R, Peddada S, Sintov A, Brodsky B, Nyska A. Reduced sulfur mustard-induced skin toxicity in cyclooxygenase-2 knockout and celecoxib-treated mice. Toxicol Appl Pharmacol 2004a;200:40–47. [PubMed: 15451306]

Wormser U, Sintov A, Brodsky B, Casillas RP, Nyska A. Protective effect of topical iodine containing anti-inflammatory drugs against sulfur mustard-induced skin lesions. Arch Toxicol 2004b;78:156–166. [PubMed: 14618300]

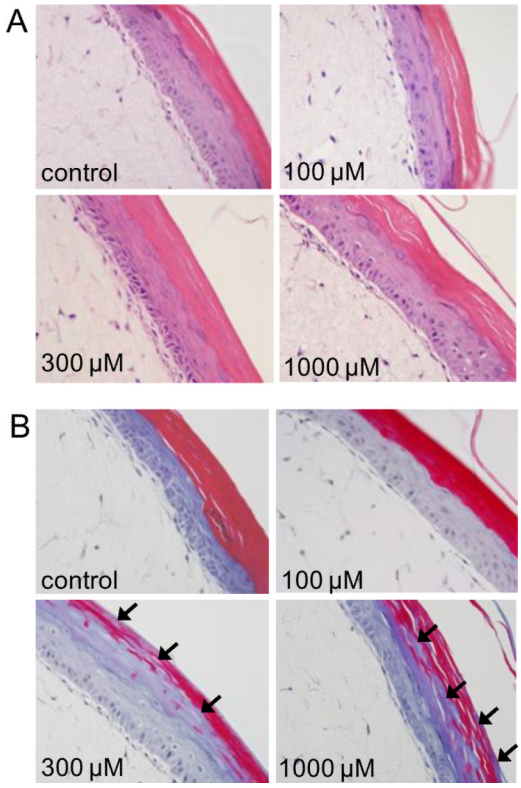

Fig. 1. Morphologic changes in full-thickness human skin equivalents following CEES treatment

EpiDerm-FT™ was treated with CEES (100–1000 μM) or vehicle control. After 24 hr, tissue samples were stained with hematoxylin and eosin (*Panel A*) or trichrome (*Panel B*). Arrows indicate abnormal trichrome staining in the stratum corneum. Original magnification, 400×.

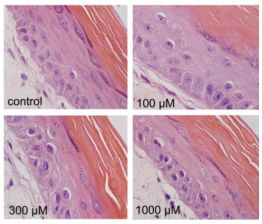

Fig. 2. Alterations in basal keratinocytes in a full-thickness human skin equivalent following CEES treatment

EpiDerm-FT™ was treated with CEES (100–1000 μM) or vehicle control. After 24 hr, tissue samples were stained with hematoxylin and eosin. Note the prominent nuclear condensation in basal keratinocytes following exposure to 300 μM and 1000 μM CEES. Original magnification, 1000×.

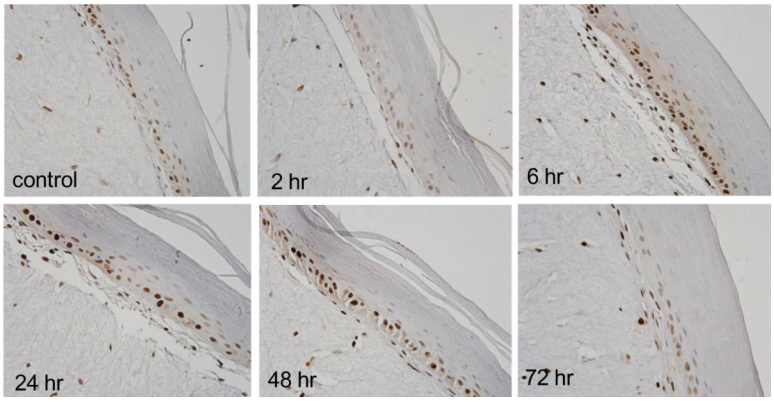

Fig. 3. Effects of CEES on PCNA expression

EpiDerm-FT™ was treated with CEES (1000 μM) or control. Tissues were collected 2–72 hr later and stained with anti-PCNA antibody. Binding was visualized using a peroxidase DAB substrate kit. Original magnification, 400×.

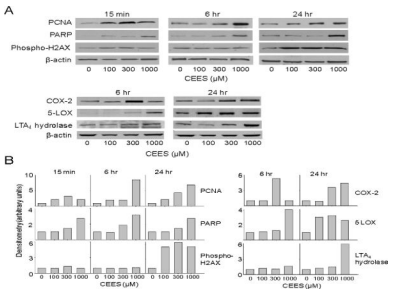

Fig. 4. Effects of CEES on expression of markers of injury and inflammation

EpiDerm-FT™ was treated with CEES (100, 300 or 1000 μM) or control for 15 min, 6 hr, or 24 hr, as indicated. *Panel A.* Epidermal sheets were collected and analyzed for protein expression by Western blotting using anti-PCNA, PARP, phospho-H2AX, COX-2, 5-LOX, and LTA_4 hydrolase antibodies. β-actin was used as a control to ensure equal protein loading. *Panel B.* Densitometry was performed on Western blots shown in Panel A. Data is presented in arbitrary units.

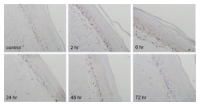

Fig. 5. Effects of CEES on PARP expression

EpiDerm-FT™ was treated with CEES (1000 μM) or control. Tissues were collected 2–72 hr later and stained with anti-PARP antibody. Binding was visualized using a peroxidase DAB substrate kit. Original magnification, 400×.

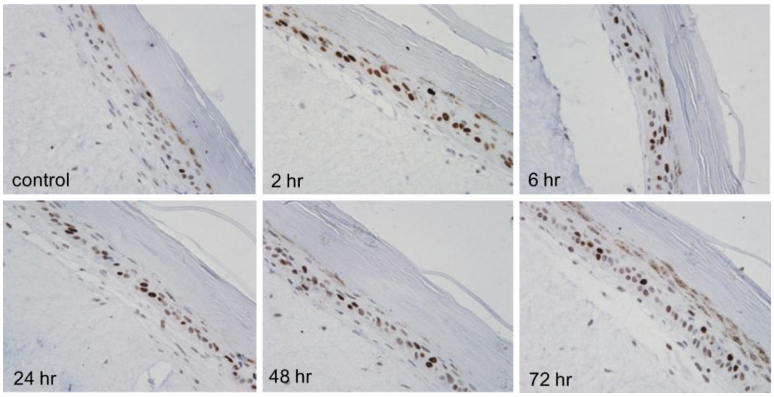

Fig. 6. Effects of CEES on phospho-H2AX expression

EpiDerm-FT™ was treated with CEES (1000 μM) or control. Tissues were collected 2–72 hr later and stained with anti-phospho-H2AX antibody. Binding was visualized using a peroxidase DAB substrate kit. Original magnification, 400×.

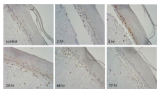

Fig. 7. Effects of CEES on COX-2 expression

EpiDerm-FT™ was treated with CEES (1000 μM) or control. Tissues were collected 2–72 hr later and stained with anti-COX-2 antibody. Binding was visualized using a peroxidase DAB substrate kit. Original magnification, 400×.

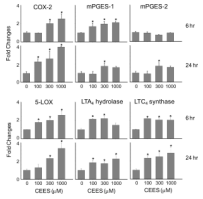

Fig. 8. Effects of CEES on mRNA expression of eicosanoid biosynthetic enzymes

EpiDerm-FT™ was treated with CEES (100, 300 or 1000 μM) or control. After 6 or 24 hr, epidermal sheets were collected and mRNA isolated and analyzed for gene expression by real-time PCR. Data are presented as fold change in gene expression relative to untreated cells. *Significantly different from control ($p < 0.05$).

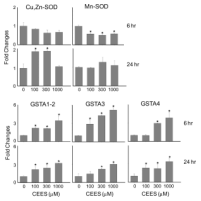

Fig. 9. Effects of CEES on keratinocyte mRNA expression of primary antioxidants and glutathione *S*-transferases

EpiDerm-FT™ was treated with CEES (100, 300 or 1000 μM) or control. After 6 or 24 hr, epidermal sheets were collected and mRNA isolated and analyzed for gene expression by real-time PCR. Data are presented as fold change in gene expression relative to untreated cells. *Significantly different from control ($p < 0.05$).